

# Effects of isothermal annealing on the microstructure and mechanical properties of SiC ceramics hot-pressed with $Y_2O_3$ and $Al_2O_3$ additions

Dong Ik Cheong<sup>a,1</sup>, Joosun Kim<sup>b</sup>, Suk-Joong L. Kang<sup>a,\*</sup>

<sup>a</sup>Materials Interface Laboratory, Department of Materials Science and Engineering, Korea Advanced Institute of Science and Technology, Taejeon, 305-701 South Korea

<sup>b</sup>Nano-Materials Research Center, Korea Institute of Science and Technology, Seoul, 130-650 South Korea

Received 31 January 2001; received in revised form 30 August 2001; accepted 19 September 2001

## Abstract

Silicon carbide compacts containing various  $\alpha$  contents and 7 wt.% of  $Y_2O_3$  and  $Al_2O_3$  (weight ratio 60:40) were hot-pressed and isothermally annealed at 1950 °C to study the coarsening behavior of SiC grains and the crystallization of the grain-boundary glass phase. The samples which were prepared from the powder compacts containing small amounts of the  $\alpha$  phase contained well-developed large plate-like grains in fine matrix grains and showed enhanced fracture toughness. A subsequent isothermal annealing was effective in controlling the grain boundary phase and resulted in the enhancement of mechanical properties. When the crystallization of the grain boundary phase leads to an aluminum-rich phase (Y–Al garnet) during the intermediate stage of annealing, flexural strength is improved. On the other hand, the fracture toughness can be increased when crystallization of the grain boundary glass is directed to an yttrium-rich phase during extended annealing. These results were explained in terms of the thermal mismatch between the SiC grain and the remaining glassy phase. © 2002 Elsevier Science Ltd. All rights reserved.

**Keywords:** Crystallization; Grain boundaries; Mechanical properties; Microstructure-final; SiC

## 1. Introduction

Liquid-phase sintered silicon carbide ceramics have a high potential for applicability in structural parts; nevertheless, their application is still restricted by their low fracture resistance. During the last decade, several attempts have been made to improve the fracture toughness of SiC ceramics.<sup>1–10</sup> Among them, a technique of microstructure control, which obtains a bimodal grain size distribution, has been quite successful. The technique utilizes the phase transformation from  $\beta$ -(a cubic phase) to  $\alpha$ -SiC (a hexagonal phase) and subsequent grain growth to form large plate-like grains in fine matrix grains.<sup>1–7</sup> The anisotropic growth nature of  $\alpha$ -SiC grains is now known to be responsible for the

formation of elongated plate-like grains in the fine matrix.<sup>7,11</sup> When large  $\alpha$ -SiC seed particles were added to  $\beta$ -SiC starting powder, such a duplex microstructure was easy to obtain. However, in solid state sintering, the seed particle addition usually resulted in a porous microstructure, <80% of the theoretical density, because of the rigid network formation of the elongated  $\alpha$ -SiC grains.<sup>12</sup>

A weak interface was thought to be prerequisite for activating toughening mechanisms, such as crack deflection and grain bridging, which contribute to enhanced energy dissipation upon crack propagation.<sup>4,5,9,10,13</sup> An elongated grain structure coupled with inter-granular fracture, in fact, led to an enhanced fracture toughness of SiC ceramics. Tajima et al.<sup>14</sup> reported that between two kinds of in situ toughened  $Si_3N_4$  materials with similar microstructures but different second phase chemistry, only the material which fractured inter-granularly exhibited bridging grains in the crack tip wake and, therefore, an increased fracture toughness. We also observed that the formation of plate-like grains using mixtures of  $\alpha$ - and  $\beta$ -SiC with an  $Al_2O_3$  addition did not

<sup>1</sup> Currently with the Agency for Defense Development, Taejeon, 350-600 South Korea.

\* Corresponding author. Tel.: +82-42-869-4113; fax: +82-42-869-8920.

E-mail address: sjkang@mail.kaist.ac.kr (S.-J.L. Kang).

result in an improvement of fracture toughness when there was a high resistance to crack propagation along grain boundaries.<sup>15</sup>

In the present work, based on the concept of seeding and growth, the effects of the initial  $\alpha$  phase content on the microstructural development and mechanical properties of liquid-phase sintered silicon carbide ceramics were studied. Appropriate sintering temperatures and refractory additive composition were selected to suppress homogeneous nucleation and grain growth during annealing. Enhancement of mechanical properties by prolonged isothermal annealing has been discussed in relation to microstructural changes, including the crystallization of the grain boundary phase.

## 2. Experimental procedure

Samples were prepared from  $\alpha$ -SiC (A10, H. C. Starck, Germany),  $\beta$ -SiC (B10, H. C. Starck),  $\text{Al}_2\text{O}_3$  (99.9%, Sumitomo Chemicals, Tokyo, Japan) and  $\text{Y}_2\text{O}_3$  (HS, H.C. Stark, Germany) powders. According to the producer's data, the FSSS (Fisher Sub-Sieve Sizer) particle sizes of the  $\alpha$ - and  $\beta$ -SiC powders were 0.8 and 0.7  $\mu\text{m}$ , respectively, and the free silicon contents were less than 0.1 wt.%. Five kinds of powder mixtures were prepared, each containing 93 wt.% of SiC ( $\alpha$  and/or  $\beta$ ) and 7wt.% of  $\text{Y}_2\text{O}_3$  and  $\text{Al}_2\text{O}_3$  (weight ratio 60:40). The ratios of  $\alpha$  to  $\beta$  in the starting powder mixtures were 0/100, 5/95, 10/90, 20/80, and 100/0. Compared with  $\text{YAG}(\text{3Y}_2\text{O}_3 \cdot 5\text{Al}_2\text{O}_3)$ -based common additive, an  $\text{Al}_2\text{O}_3$ -rich one,<sup>5,11,12</sup> the selected additive composition is  $\text{Y}_2\text{O}_3$ -rich. With this composition, we may expect a higher formation temperature<sup>16</sup> and a higher viscosity of liquid.

Each batch was ball-milled for 12 h in a polyethylene bottle with alumina balls and ethyl alcohol. The dried slurry was granulated using a 120 mesh sieve. Each granulated powder mixture of approximately 30 g was hot-pressed under 30 MPa in a graphite furnace at 1950 °C for 2 h in Ar to a plate of 40×40×6 mm. During the hot pressing, the heating rate was 30 K/min. To promote the grain growth and crystallize the grain boundary phase, the hot-pressed samples were pressurelessly annealed at 1950 °C for 2, 4 or 6 h in Ar using the graphite furnace for hot pressing.

The sintered density was measured by the Archimedes method. The theoretical density of the samples was taken to be 3.28 g/cm<sup>3</sup>, a value obtained using the rule of mixture. The microstructures of the samples were observed using a scanning electron microscope (SEM) on their cross-sections after polishing and etching with a plasma of 7.8%- $\text{O}_2$  containing  $\text{CF}_4$ . The equivalent diameter of each grain was measured by the areal analysis technique using ANALYSYS (Soft-Imaging Software Corp., Germany). Over 900 grains were measured for the determination of the grain size distribution. For

phase identification, X-ray diffraction using  $\text{Cu-K}\alpha$  radiation was performed on the polished sample surfaces. Transmission electron microscope (TEM) with energy dispersive spectroscopy (EDS) was also used to study the crystallization of the grain boundary phase during annealing.

Fracture toughness was measured by the single edge pre-cracked beam (SEPB) method according to KS L 1600<sup>17</sup> for specimens of 4×3×19 mm. A pre-crack was introduced at the center of the specimen in a direction parallel to the hot-pressing direction. Three-point loading with a span of 16 mm was applied. The fracture toughness value was calculated using the following equation:

$$K_{\text{IC}} = \left( \frac{PS}{BW^{3/2}} \right) \left\{ \frac{3}{2} \left( \frac{a}{W} \right)^{1/2} \cdot Y \left( \frac{a}{W} \right) \right\}, \quad (1)$$

where  $K_{\text{IC}}$  is the fracture toughness,  $P$  the peak load in the load-displacement diagram,  $S$  the span of the load bearing point (16 mm),  $B$  the width of the specimen (3 mm),  $W$  the thickness of the specimen (4 mm), and  $a$  the average crack length. The shape factor  $Y$  was calculated from the following equation.

$$Y = \frac{W}{a} \times \frac{\left[ 1.99 - \frac{a}{W} \cdot \left( 1 - \frac{a}{W} \right) \cdot \left\{ 2.15 - 3.93 \cdot \frac{a}{W} + 2.7 \cdot \left( \frac{a}{W} \right)^2 \right\} \right]}{\left( 1 + 2 \cdot \frac{a}{W} \right) \cdot \left( 1 - \frac{a}{W} \right)^{3/2}}. \quad (2)$$

Four-point flexural strength was measured with test bars of 4×3×40 mm using an inner and outer span of 10 and 30 mm, respectively, with a crosshead speed of 0.5 mm/min. Seven specimens were tested for each processing condition.

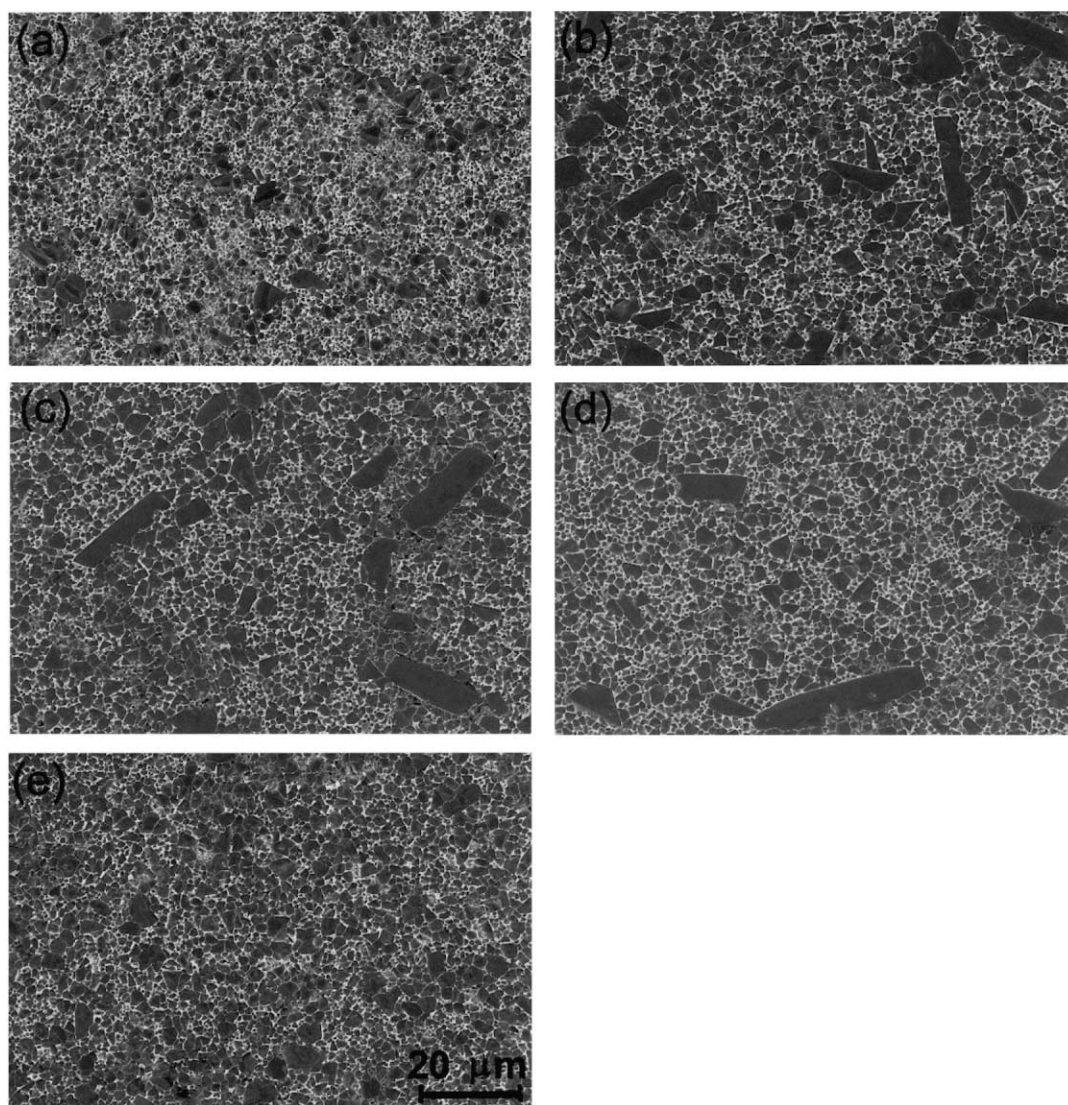
## 3. Results and discussion

After the hot pressing, all of the samples were densified to over 98% of the theoretical value and consisted of fine and equiaxed SiC grains. However, the phases present in the samples were different according to  $\alpha$ - to  $\beta$ -SiC ratios in the powder mixtures, as listed in Table 1. When these samples were annealed at 1950 °C, the microstructures varied with the  $\alpha$ - to  $\beta$ -SiC ratios in the starting powder mixtures, as shown in Fig. 1. In the samples made from unmixed  $\alpha$ - or  $\beta$ -SiC powders [Fig. 1(a) and (e)], few abnormal grains were present. On the other hand, in the samples made from a mixture of  $\alpha$ - $\beta$  powders [Fig. 1(b), (c) and (d)], many in situ grown large plate-like SiC grains were observed in equiaxed fine matrix grains, showing a bimodal grain size distribution. These microstructural characteristics were maintained

Table 1

Relative density and phase assemblage of the samples hot-pressed at 1950 °C for 2 h with different  $\alpha$ - to  $\beta$ -SiC ratios in the starting powder

Specimen ( $\alpha/\beta$ )	Batch composition (wt.%)				Relative density <sup>a</sup> (%)	Phase assemblage	
	$\alpha$ -SiC	$\beta$ -SiC	Y <sub>2</sub> O <sub>3</sub>	Al <sub>2</sub> O <sub>3</sub>		Major	Trace
0/100	0.0	93.0	4.2	2.8	98.4	3C	6H
5/95	4.6	88.4	4.2	2.8	98.3	3C, 6H	15R
10/90	9.3	83.7	4.2	2.8	98.3	3C, 6H	15R
20/80	18.6	74.4	4.2	2.8	98.3	3C, 6H	15R
100/0	93.0	0.0	4.2	2.8	98.7	6H	15R

<sup>a</sup> Calculated theoretical density: 3.28 g/cm<sup>3</sup>.Fig.1. SEM micrographs of SiC samples hot-pressed and subsequently annealed at 1950 °C for 2 h. Samples were prepared from powders of different ratios of  $\alpha$  to  $\beta$ -SiC: (a) 0/100, (b) 5/95, (c) 10/90, (d) 20/80, and (e) 100/0.

during extended annealing (Fig. 2). In the samples prepared from unmixed ( $\alpha$  or  $\beta$ ) powders, no abnormal grain growth occurred, but a slight increase in the average grain size resulted with an increase of annealing time

[for example, Fig. 2(a)] showing a normal grain growth behavior. In the samples made from mixed powders [Fig. 2(b)], however, the large plate-like grains grew at the expense of small matrix grains.

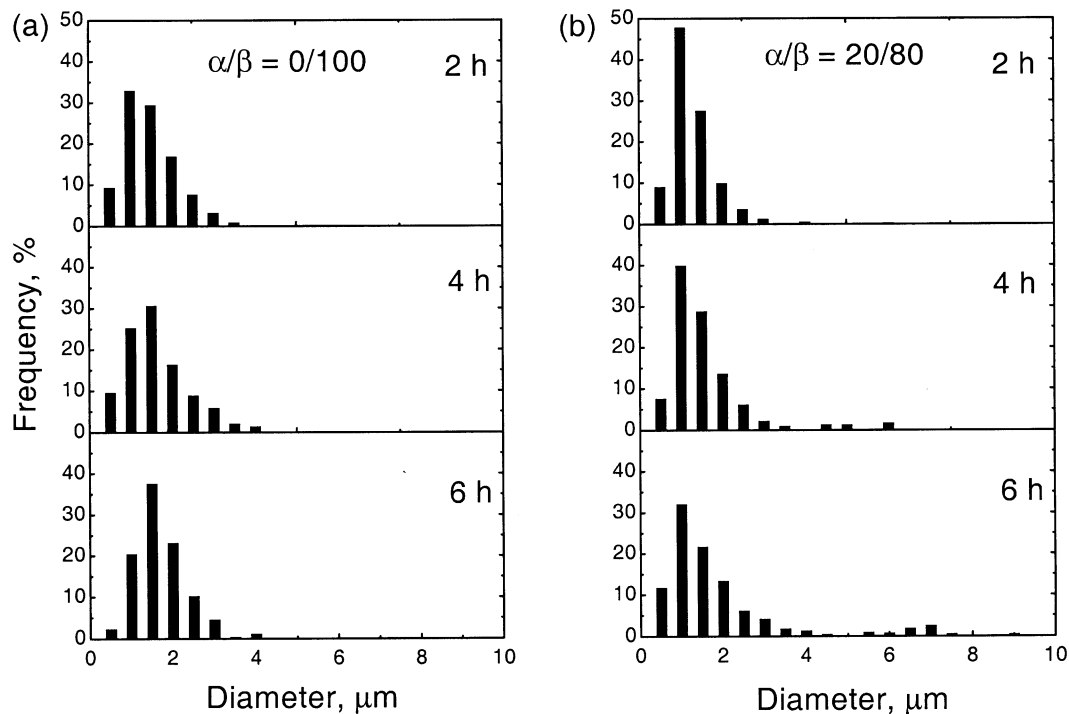


Fig. 2. Grain size distributions of samples with an  $\alpha$  to  $\beta$ -SiC ratio of (a) 0/100 and (b) 20/80 in the starting powder. The samples were annealed at 1950 °C for the noted period of time.

The presence of large plate-like grains ( $> 7 \mu\text{m}$ ) in the sample prepared from  $\alpha + \beta$  mixed powders shows that an 'in situ composite microstructure' was developed as a result of subsequent annealing. This result is consistent with previous ones,<sup>3,6,8</sup> which also showed the formation of in situ composites by the seeding of small amounts of  $\alpha$ -SiC particles into a fine  $\beta$ -SiC powder batch.

Fig. 3 plots the measured flexural strengths of various samples as a function of the phase ratio in the starting powders and annealing time. Independent of the annealing time, minimum strengths emerge for  $\sim 10\%$   $\alpha$ -SiC-contained samples in the starting powder mixture. This result suggests that strength degradation is closely related to the presence of large plate-like grains as found in previous investigations of in situ toughened ceramics.<sup>1</sup> In the case of silicon nitride-based ceramics, the strength decreases when large elongated grains are present in fine matrix grains.<sup>18,19</sup>

The flexural strengths of the samples annealed for 4 h in Fig. 3, however, appear to be superior to those of the samples annealed for 2 or 6 h. Since the sizes of average grains as well as abnormal grains increase as the annealing time increases, the strength is expected to decrease when increasing the annealing time from 2 to 4 h, in contrast to the present measurement for the 2 and 4 h-annealed samples. The observed superior strengths of the 4 h-annealed samples may be due to possible change in interface strength between SiC grains and the surrounding liquid phase during the annealing. The variation in strength with annealing time would then be

a result of the change in grain boundary chemistry as well as grain size.

Comparing the flexural strengths of the samples from 100%  $\alpha$ - and 100%  $\beta$ -SiC powders, the sample from  $\alpha$  powder has a higher strength than that from  $\beta$  powder. As shown in Table 1, there was essentially no phase transformation from the starting phases. In addition,

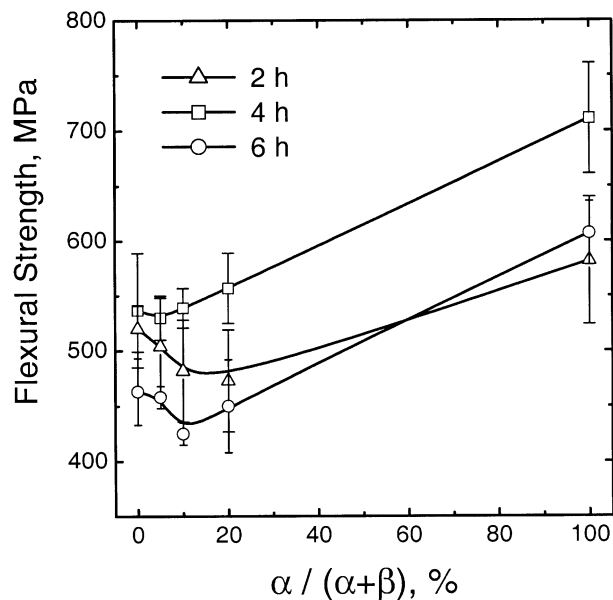


Fig. 3. Variation of flexural strengths of samples hot-pressed and annealed at 1950 °C for various periods of time as a function of the phase ratio in the starting powder.

the average grain sizes of the two different samples are similar. It appears, therefore, that the difference in flexural strength between the samples is due to the difference in crystalline phase. According to a previous investigation,<sup>20</sup> the Young's moduli of  $\alpha$ - and  $\beta$ -SiC whiskers are 190 and 380–650 GPa, respectively. The higher flexural strength of the sample from 100%  $\alpha$ -SiC powder seems to be related to the higher modulus.

Fig. 4 shows the variation of fracture toughness as a function of the phase ratio in the starting powders and annealing time. The toughness increases with annealing time, and reaches the maximum for the sample prepared from a 20 $\alpha$ /80 $\beta$  powder mixture and annealed for 6 h. It is probable that the large plate-like abnormal grains in the samples improved the fracture toughness, as in the case of  $\text{Si}_3\text{N}_4$  ceramics.<sup>18,19,21</sup> In our previous investigation,<sup>15</sup> however, the fracture toughness of  $\text{Al}_2\text{O}_3$ -added SiC decreased in spite of the presence of large elongated grains due to a transgranular fracture, which suggests the importance of the interface property. To achieve high fracture toughness in SiC ceramics, therefore, it appears necessary that (i) large plate-like grains are included in the material with fine grains and, (ii) at the same time, the interface between the grain and the matrix phase is weak to induce the crack deflection.<sup>5,15</sup>

The observed variations in flexural strength and fracture toughness with annealing time would then be understood in terms of the variation in the grain boundary phase. A grain boundary phase is usually present as a meta-stable glass phase for thermodynamic and kinetic reasons which are related to the geometrical criteria.<sup>22</sup> Upon suitable annealing, however, the grain-boundary glass phase can crystallize to a great extent.

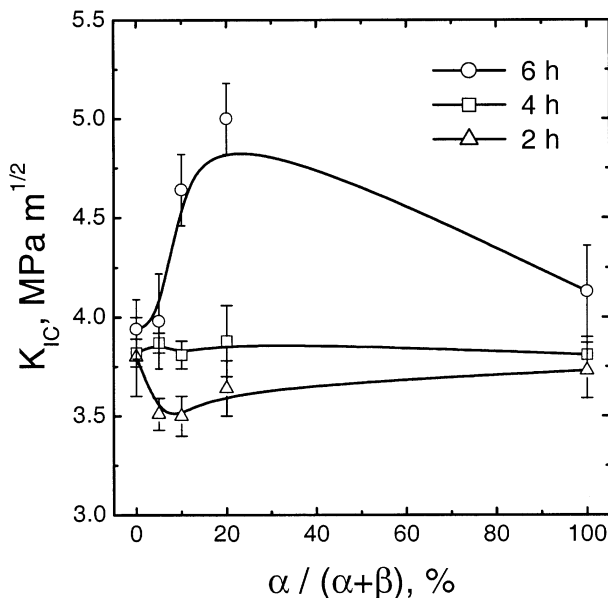


Fig. 4. Variation of fracture toughnesses of samples hot-pressed and annealed at 1950 °C for various periods of time as a function of the phase ratio in the starting powder.

The materials then become multiphase: SiC grains, a glassy phase, and crystalline second phases. The X-ray diffraction spectra in Fig. 5 reveal such grain boundary crystallization. The sample annealed for 4 h contains a garnet ( $\text{Y}_3\text{Al}_5\text{O}_{12}$ ) phase. In the sample annealed for 6 h, however, not only the garnet-phase but also a high yttrium ( $\text{YAlO}_3$ ) phase are present. A TEM observation and compositional analysis by EDS confirmed the crystallization of a grain boundary glass phase, as shown in Fig. 6. The sample hot-pressed for 2 h did not contain any detectable crystalline second phase, but only yttrium containing aluminosilicate glasses at the SiC grain interface or junction.

The crystallization of a garnet phase reduces the Al content in the remaining glass phase and contributes to reducing the residual stresses arising from the thermal expansion mismatch between SiC and the grain boundary glass phase.<sup>23</sup> As the alumina content decreases in the yttrium containing aluminosilicate glass with its crystallization, the thermal expansion coefficient of the glass becomes close to that of SiC. The reduction of residual stresses with the crystallization might contribute to maintaining high flexural strength and decreasing fracture toughness because of the improvement in interface strength. Upon prolonged annealing, however, the crystallization of the yttrium-rich grain-boundary phase considerably reduces the yttrium content in the remaining glass, which can result in high thermal expansion mismatch at the grain interface.<sup>23</sup> This thermal expansion mismatch might produce micro-cracks or a weak interface, and therefore, contribute to the enhancement of fracture toughness via crack bridging and deflection, as observed in the present investigation.

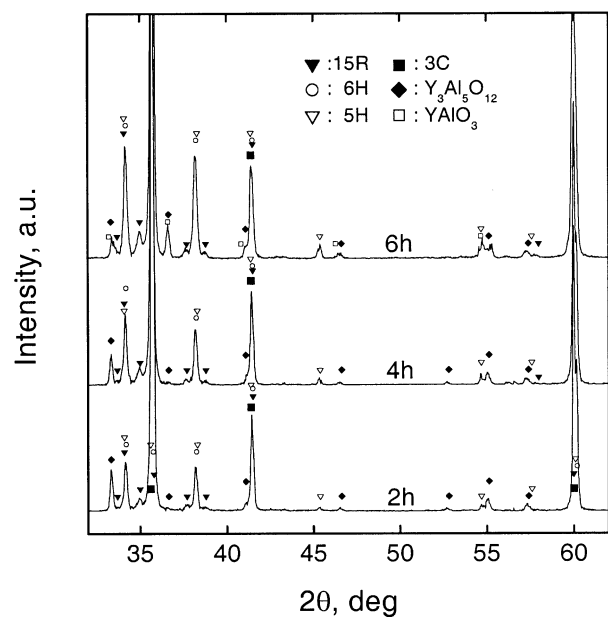


Fig. 5. X-ray diffraction spectra of the 20 $\alpha$ /80 $\beta$  samples hot-pressed and annealed at 1950 °C for various periods of time.

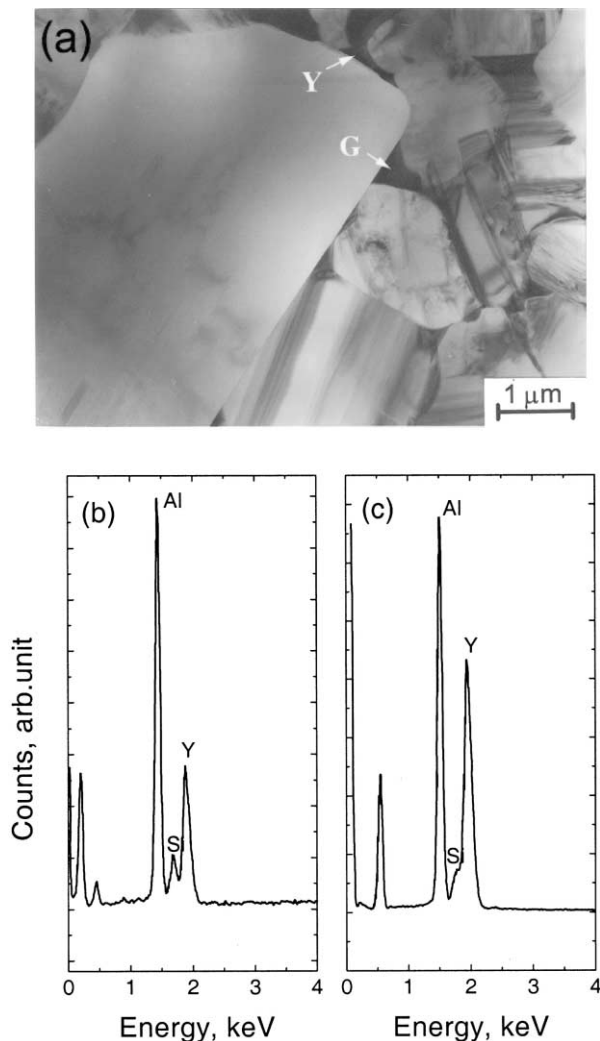


Fig. 6. (a) TEM micrograph of the 20 $\alpha$ /80 $\beta$  sample hot-pressed and annealed at 1950 °C for 6 h; (b) and (c) EDS spectra of junction “G” (b) and “Y” (c), respectively. “G” denotes a garnet phase and “Y” a yttrium-rich phase.

#### 4. Conclusions

Silicon carbide powders with various  $\alpha$ - to  $\beta$ -SiC ratios in the initial powder mixture and 7 wt.%  $\text{Y}_2\text{O}_3$  and  $\text{Al}_2\text{O}_3$  (weight ratio 60:40) additives were hot-pressed and isothermally annealed. In the samples prepared from  $\alpha$ - and  $\beta$ -SiC mixed powders, large plate-like grains formed during subsequent isothermal annealing, which resulted in a bimodal grain size distribution. The grain boundary glass phase crystallized into a YAG and an yttrium-rich phase during extended isothermal annealing. When crystallization is directed to formation of the YAG phase, the flexural strength increased. However, when the yttrium-rich phase was formed during crystallization, fracture toughness enhancement was pronounced. These results could be explained in terms of the thermal mismatch between SiC grains and the

remaining glass phase during annealing. In short, crystallization control of the grain boundary phase seems to be a key for mechanical property improvement along with the microstructure control in silicon carbide ceramics hot-pressed with  $\text{Y}_2\text{O}_3$  and  $\text{Al}_2\text{O}_3$  additives.

#### References

1. Padture, N. P., In situ toughened silicon carbide. *J. Am. Ceram. Soc.*, 1994, **77**, 519–523.
2. Padture, N. P. and Lawn, B. R., Toughness properties of a silicon carbide with an in situ induced heterogeneous grain structure. *J. Am. Ceram. Soc.*, 1994, **77**, 2518–2522.
3. Mitchell Jr., T., DeJonghe, L. C., MoberlyChan, W. J. and Ritchie, R. O., Silicon carbide platelet/silicon carbide composites. *J. Am. Ceram. Soc.*, 1995, **78**, 97–103.
4. Cao, J. J., MoberlyChan, W. J., DeJonghe, L. C., Gilbert, C. J. and Ritchie, R. O., In situ toughened silicon carbide with Al–B–C additions. *J. Am. Ceram. Soc.*, 1996, **79**, 461–469.
5. Kim, J. Y., Kim, Y. W., Mitomo, M., Zhan, G.-D. and Lee, J. G., Microstructure and mechanical properties of alpha-silicon carbide sintered with yttrium-aluminum garnet and silica. *J. Am. Ceram. Soc.*, 1999, **82**, 441–444.
6. Han, S. M., Lee, S. M. and Kang, S.-J. L., Phase transformation and microstructure development in silicon nitride based materials. In *Advanced Materials '93: Ceramics, Powders, Corrosion, and Advanced Processing*, ed. N. Mizutani et al. Elsevier Science, Amsterdam, 1994, pp. 851–856.
7. MoberlyChan, W. J., Cao, J. J., Gilbert, C. J., Ritchie, R. O. and DeJonghe, L. C., The cubic-to-hexagonal transformation to toughen SiC. In *Ceramic Microstructures: Control at the Atomic Level*, ed. A. P. Tomisa and A. Glaeser. Plenum Press, New York, 1998, pp. 177–190.
8. Forster, J., Vassen, R. and Stover, D., Improvement of fracture toughness in hot isostatically pressed mixtures of ultrafine and coarse grained SiC ceramics. *J. Mater. Sci. Lett.*, 1995, **14**, 214–216.
9. MoberlyChan, W. J. and DeJonghe, L. C., Controlling interface chemistry and structure to process and toughen silicon-carbide. *Acta Mater.*, 1998, **46**, 2471–2477.
10. MoberlyChan, W. J., Cao, J. J. and DeJonghe, L. C., The role of amorphous grain boundaries and the  $\beta \rightarrow \alpha$  transformation in toughening SiC. *Acta Mater.*, 1998, **46**, 1625–1635.
11. Ogbuji, L. U., Michelle, T. E., Heuer, A. H. and Shinozaki, S., The  $\beta \rightarrow \alpha$  Transformation in polycrystalline SiC: IV, a comparison of conventionally sintered, hot-pressed, reaction-sintered, and chemically vapor-deposited samples. *J. Am. Ceram. Soc.*, 1981, **64**, 91–99.
12. Johnson, C. A. and Prochazka, S., Microstructure of sintered SiC. In *Ceramic Microstructures '76*, ed. R. M. Fulrath and J. A. Pask. Westview Press, Boulder, 1977, pp. 366–378.
13. Kleebe, H.-J., Pezzotti, G. and Ziegler, G., Microstructure and fracture toughness of  $\text{Si}_3\text{N}_4$  ceramics: combined roles of grain morphology and secondary phase chemistry. *J. Am. Ceram. Soc.*, 1999, **82**, 1857–1867.
14. Tajima, Y., Urashima, K., Watanabe, M. and Matsuo, Y., Fracture toughness and microstructure evaluation of silicon nitride ceramics. In *Ceramic Transactions, Vol. 1; Ceramic Powder Science-II*, ed. G. L. Messing, E. R. Fuller, Jr. and H. Hausner. American Ceramic Society, Westerville, OH, 1988, pp. 1034–1041.
15. Cheong, D. I., Kang, E. S., Baek, Y. K. and Kang, S.-J. L., Effect of  $\alpha/\beta$  ratio in starting powder mixture on microstructure and mechanical properties of hot-pressed 98.5SiC–1.5Al $_2$ O $_3$ . In *Proceedings of The Fourth Conference of the European Ceramic Society*, Vol. 3, 1995, pp. 487–492.

16. Toropov, N. A., Fig. 2344 (phase diagram of  $Y_2O_3$ – $Al_2O_3$ ). In *Phase Diagram for Ceramists*, Vol. 2, ed. E. M. Levin, C. R. Robbins and H. F. McMurdie. American Ceramic Society, Westerville, OH, 1964, pp. 96.
17. KS L 1600, Testing Methods for Fracture Toughness of High Performance Ceramics. Korea Standards Association, 1995.
18. Lange, F. F., Relation between strength, fracture energy, and microstructure of hot-pressed  $Si_3N_4$ . *J. Am. Ceram. Soc.*, 1973, **56**, 518–522.
19. Kim, J. S., Rosenflanz, A. and Chen, I.-W., Microstructure control of in situ toughened  $\alpha$ -SiAlON ceramics. *J. Am. Ceram. Soc.*, 2000, **83**, 1819–1821.
20. *Engineering Property Data on Selected Ceramics*, Vol 2; *Carbides, Metals and Ceramics*. Information Center, Columbus, OH, 1979, pp. 5.2.3–9.
21. Hirao, K., Tsuge, A., Brito, M. E. and Kanzaki, S., Microstructure control of silicon nitride by seeding with rodlike  $\beta$ -silicon nitride particles. *J. Am. Ceram. Soc.*, 1994, **77**, 1857–1862.
22. Clarke, D. R., On the equilibrium thickness of intergranular glass phase in ceramic materials. *J. Am. Ceram. Soc.*, 1987, **70**, 15–22.
23. Hyatt, M. J. and Day, D. E., Glass properties in the yttria-alumina-silica system. *J. Am. Ceram. Soc.*, 1987, **70**, C283–C287.